Supporting Information for:

GTP Hydrolysis Without an Active Site Base:

A Unifying Mechanism for Ras and Related GTPases

Ana R. Calixto[1,‡], Cátia Moreira[1,‡], Anna Pabis[2], Carsten Kötting[3], Klaus Gerwert[3], Till Rudack[3,*] and Shina C. L. Kamerlin[1,*]

1. Department of Chemistry – BMC, Uppsala University, Box 576, S-751 23 Uppsala, Sweden. 2. Department of Cell and Molecular Biology, Uppsala University, BMC Box 596, S-751 24 Uppsala, Sweden. 3. Department of Biophysics, Ruhr University Bochum, 44801 Bochum, Germany.

[‡] These authors contributed equally.

Corresponding author email addresses: till.rudack@rub.de and lynn.kamerlin@kemi.uu.se

Table of Contents

S1. Supplementary Figures

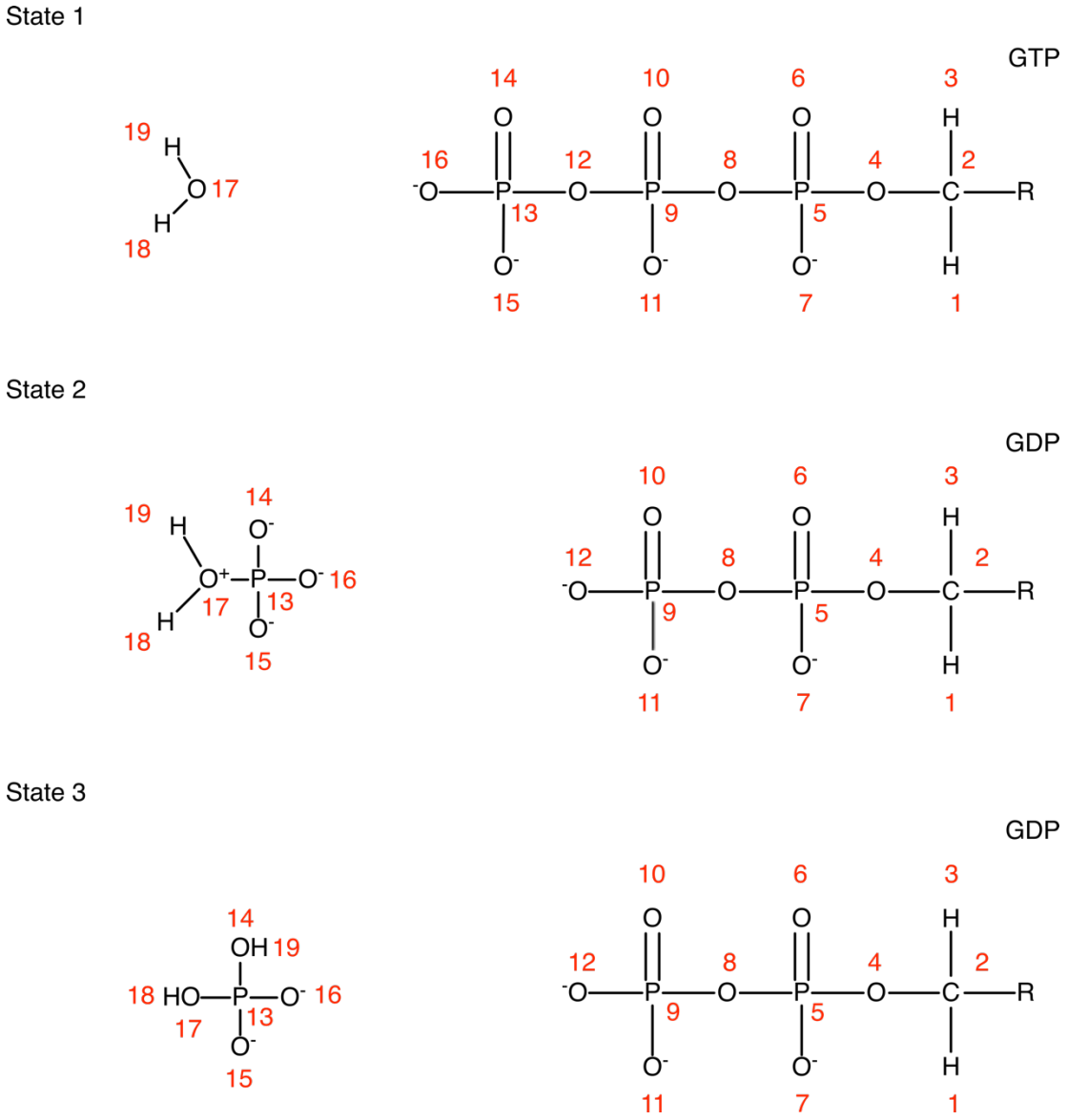

Figure S1. The valence bond states used to describe the solvent-assisted mechanism in our empirical valence bond (EVB) simulations of both the GTPase-catalyzed and non-enzymatic hydrolysis of GTP in aqueous solution and in the relevant enzyme active sites. For clarity, only the triphosphate of the GTP is indicated in this figure, as the remainder of the molecule was not part of the EVB region during our simulations. The atom numbering corresponds to the EVB parameter tables, shown in **Tables S15** to **S29**.

State 1

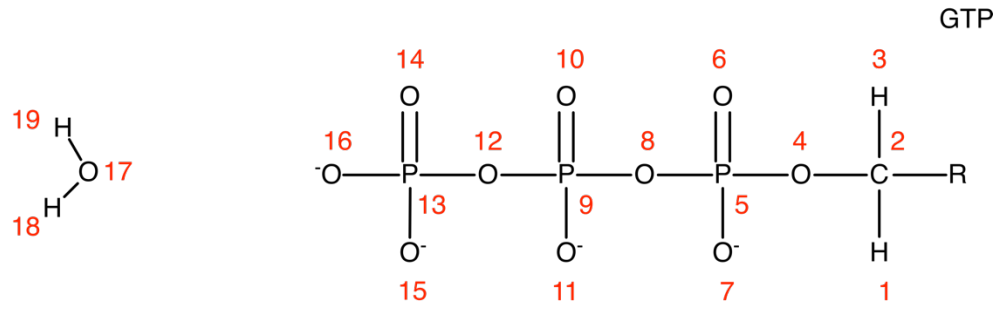

State 2

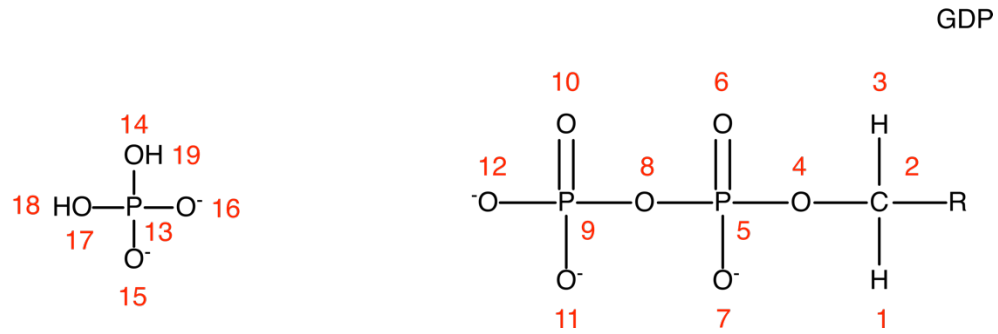

Figure S2. The valence bond states used to describe the substrate-assisted mechanism in our empirical valence bond (EVB) simulations of both the GTPase-catalyzed and non-enzymatic hydrolysis of GTP in aqueous solution and in the relevant enzyme active sites. For clarity, only the triphosphate of the GTP is indicated in this figure, as the remainder of the molecule was not part of the EVB region during our simulations. The atom numbering corresponds to the EVB parameter tables, shown in **Tables S15** to **S29**.

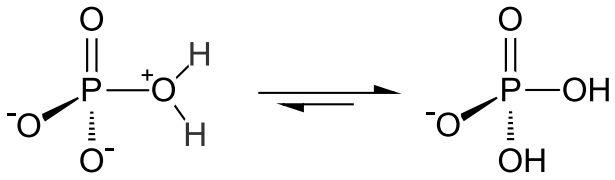

Figure S3. Transient intermediate formed during the solvent-assisted hydrolysis of GTP (left), which is expected to quickly tautomerize to form the more stable final product (right).[1]

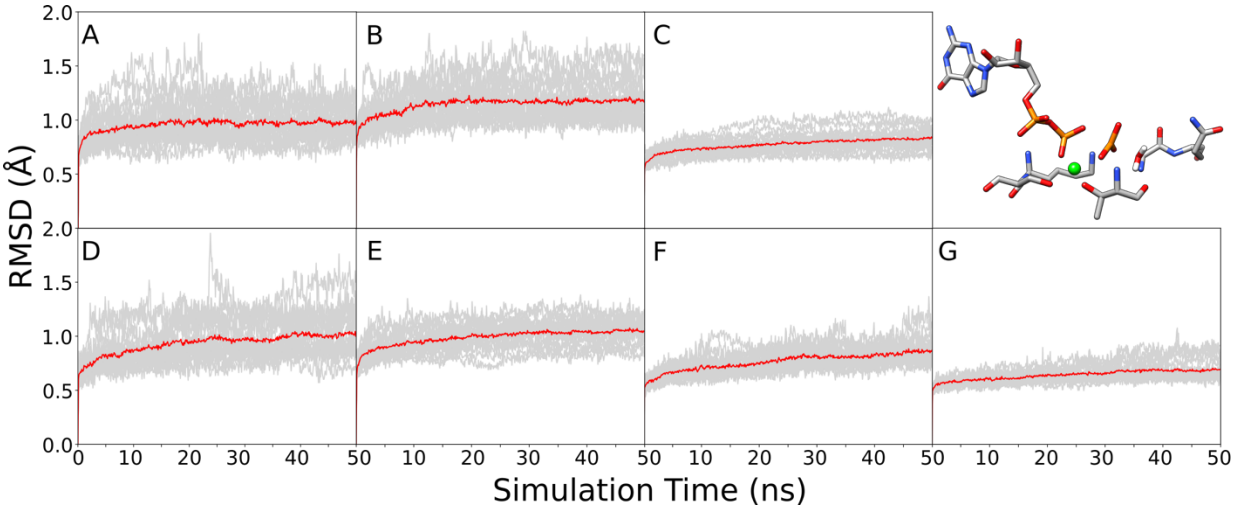

Figure S4. The root mean square deviations (RMSD, Å) of all backbone atoms during 20 x 50ns (1 μs total) of equilibration of the transition state (λ = 0.5) for the solvent-assisted hydrolysis of GTP by (**A**) wild-type Ras, (**B**) Q61H Ras, (**C**) RasGAP, (**D**) Rab, (**E**) RabGAP, (**F**) $G_{\alpha i}$ and (**G**) $G_{\alpha i}$-RGS4. Snapshots were taken every 100ps, and the RMSD values were calculated using MDtraj.[2] The grey shaded lines indicate the data from each individual trajectory for each system, and the solid red lines indicate the average RMSD over all trajectories for each system. Shown here is also a representative structure of the solvent-assisted transition state for Ras-catalyzed hydrolysis of GTP, extracted from our EVB simulations of this reaction.

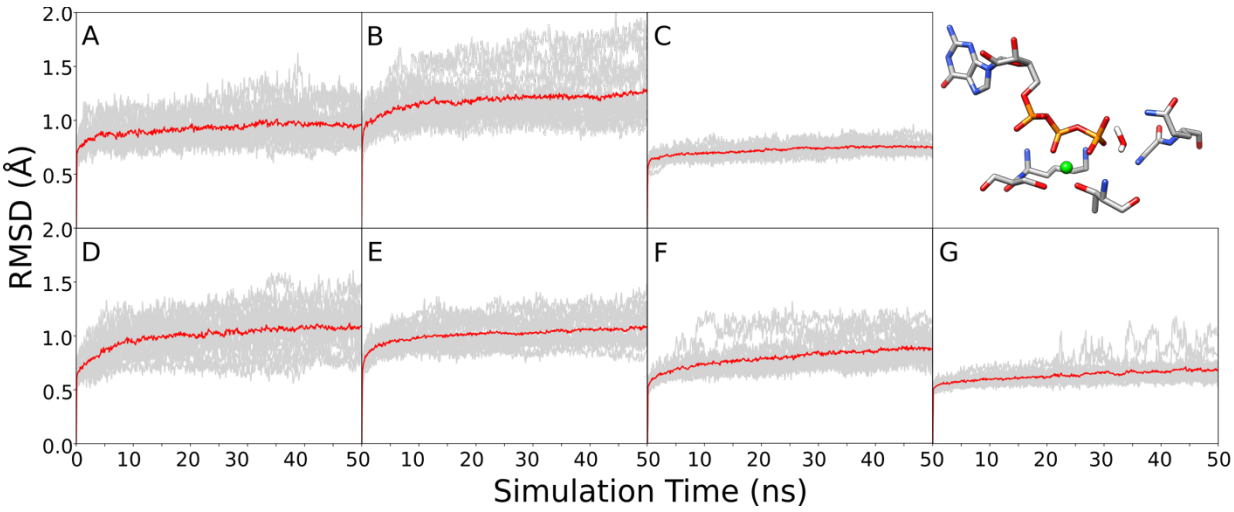

Figure S5. The root mean square deviations (RMSD, Å) of all backbone atoms during 20 x 50ns (1 μs total) of equilibration of the transition state (λ = 0.5) for the substrate-assisted hydrolysis of GTP by (**A**) wild-type Ras, (**B**) Q61H Ras, (**C**) RasGAP, (**D**) Rab, (**E**) RabGAP, (**F**) $G_{\alpha i}$ and (**G**) $G_{\alpha i}$-RGS4. Snapshots were taken every 100ps, and the RMSD values were calculated using MDtraj.[2] The grey shaded lines indicate the data from each individual trajectory for each system, and the solid red lines indicate the average RMSD over all trajectories for each system. Shown here is also a representative structure of the substrate-assisted transition state for Ras-catalyzed hydrolysis of GTP, extracted from our EVB simulations of this reaction.

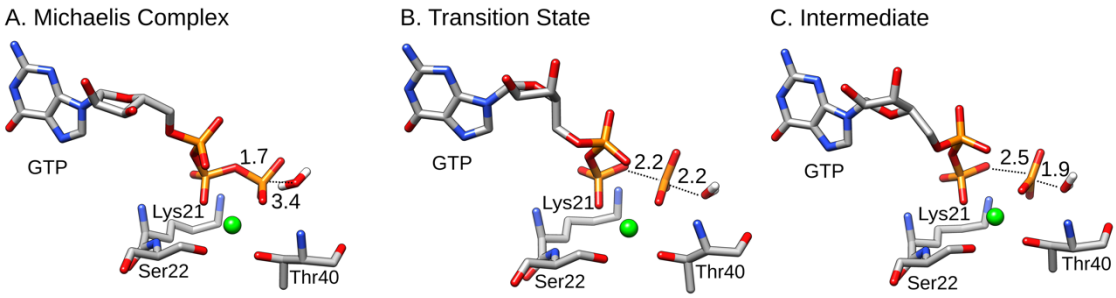

Figure S6. Structures of key stationary points, extracted from our empirical valence bond simulations of the Rab-catalyzed solvent-assisted hydrolysis of GTP. Shown here are (**A**) the Michaelis complex, (**B**) the transition state for the phosphoryl transfer reaction, and (**C**) the short-lived intermediate. Note that, as described in the main text, we only modelled the final tautomerization step (**Figure S3**) in the case of the non-enzymatic reaction, and the Ras- and RasGAP-catalyzed reactions, as this step is fast and not rate-limiting (**Figure 3**). The P-O distances annotated on this figure (in Å) are average distances over all replicas, as presented in **Table 1**, and the structures shown in this figure were selected because they have P-O distances that are very similar to the average distances across all the EVB trajectories. The corresponding free energies for this reaction can be found in **Figure 3** and **Table S3**. Shown here are the substrate, nucleophilic water molecule, Mg^{2+} ion, and key catalytic residues. The remainder of the protein has been omitted for clarity.

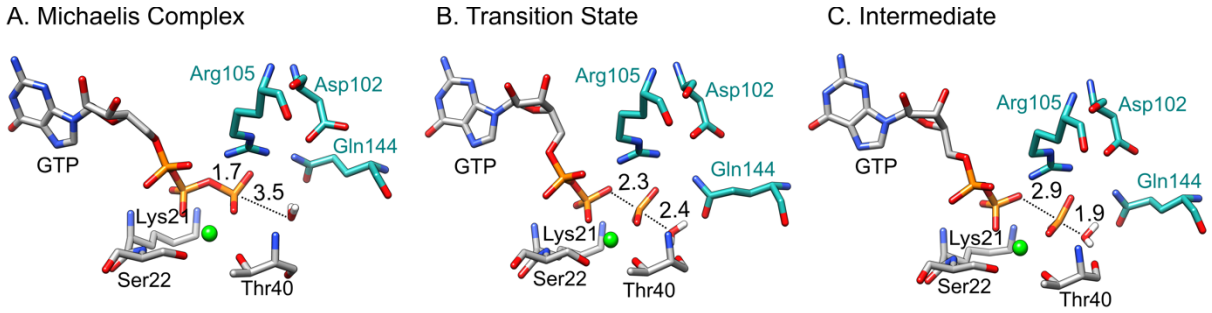

Figure S7. Structures of key stationary points, extracted from our empirical valence bond simulations of the RabGAP-catalyzed solvent-assisted hydrolysis of GTP. Shown here are (**A**) the Michaelis complex, (**B**) the transition state for the phosphoryl transfer reaction, and (**C**) the short-lived intermediate. Note that, as described in the main text, we only modelled the final tautomerization step (**Figure S3**) in the case of the non-enzymatic reaction, and the Ras- and RasGAP-catalyzed reactions, as this step is fast and not rate-limiting (**Figure 3**). The P-O distances annotated on this figure (in Å) are average distances over all replicas, as presented in **Table 1**, and the structures shown in this figure were selected because they have P-O distances that are very similar to the average distances across all the EVB trajectories. The corresponding free energies for this reaction can be found in **Figure 3** and **Table S3**. Shown here are the substrate, nucleophilic water molecule, Mg^{2+} ion, and key catalytic residues. The remainder of the protein has been omitted for clarity.

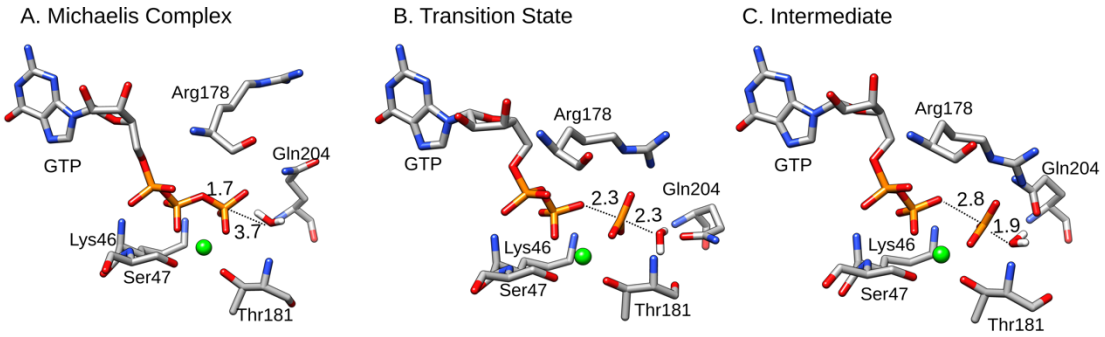

Figure S8. Structures of key stationary points, extracted from our empirical valence bond simulations of the $G_{\alpha i}$-catalyzed solvent-assisted hydrolysis of GTP. Shown here are (**A**) the Michaelis complex, (**B**) the transition state for the phosphoryl transfer reaction, and (**C**) the short-lived intermediate. Note that, as described in the main text, we only modelled the final tautomerization step (**Figure S3**) in the case of the non-enzymatic reaction, and the Ras- and RasGAP-catalyzed reactions, as this step is fast and not rate-limiting (**Figure 3**). The P-O distances annotated on this figure (in Å) are average distances over all replicas, as presented in **Table 1**, and the structures shown in this figure were selected because they have P-O distances that are very similar to the average distances across all the EVB trajectories. The corresponding free energies for this reaction can be found in **Figure 3** and **Table S3**. Shown here are the substrate, nucleophilic water molecule, Mg^{2+} ion, and key catalytic residues. The remainder of the protein has been omitted for clarity.

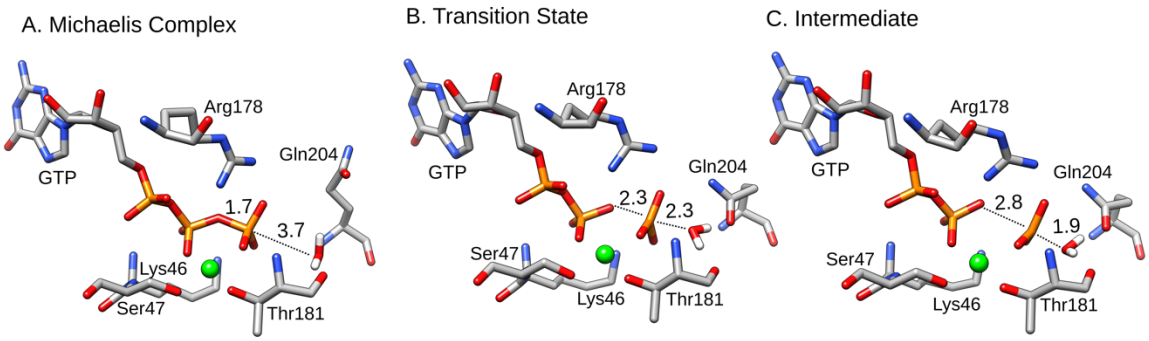

Figure S9. Structures of key stationary points, extracted from our empirical valence bond simulations of the $G_{\alpha i}$-RGS4-catalyzed solvent-assisted hydrolysis of GTP. Shown here are (**A**) the Michaelis complex, (**B**) the transition state for the phosphoryl transfer reaction, and (**C**) the short-lived intermediate. Note that, as described in the main text, we only modelled the final tautomerization step (**Figure S3**) in the case of the non-enzymatic reaction, and the Ras- and RasGAP-catalyzed reactions, as this step is fast and not rate-limiting (**Figure 3**). The P-O distances annotated on this figure (in Å) are average distances over all replicas, as presented in **Table 1** and the structures shown in this figure were selected because they have P-O distances that are very similar to the average distances across all the EVB trajectories. The corresponding free energies for this reaction can be found in **Figure 3** and **Table S3**. Shown here are the substrate, nucleophilic water molecule, Mg^{2+} ion, and key catalytic residues. The remainder of the protein has been omitted for clarity.

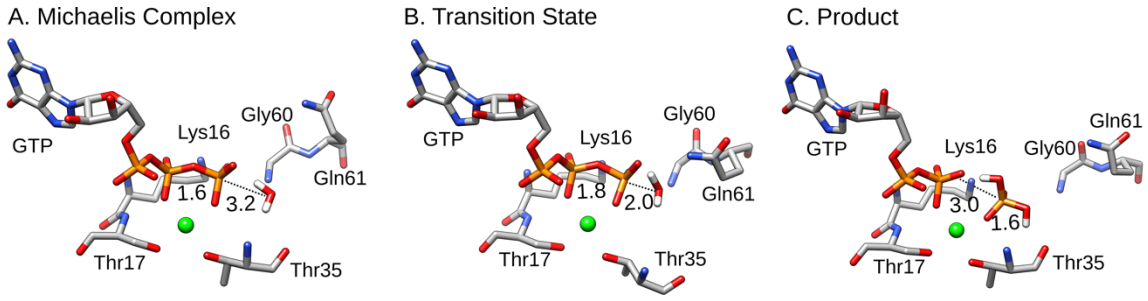

Figure S10. Structures of key stationary points, extracted from our empirical valence bond simulations of the Ras-catalyzed substrate-assisted hydrolysis of GTP. Shown here are (**A**) the Michaelis complex, (**B**) the transition state for the phosphoryl transfer reaction, and (**C**) the product complex. The P-O distances annotated on this figure (in Å) are average distances over all replicas, as presented in **Table S7**, and the structures shown in this figure were selected because they have P-O distances that are very similar to the average distances across all the EVB trajectories. The corresponding free energies for this reaction can be found in **Figure 3** and **Table S3**. Shown here are the substrate, nucleophilic water molecule, Mg^{2+} ion, and key catalytic residues. The remainder of the protein has been omitted for clarity.

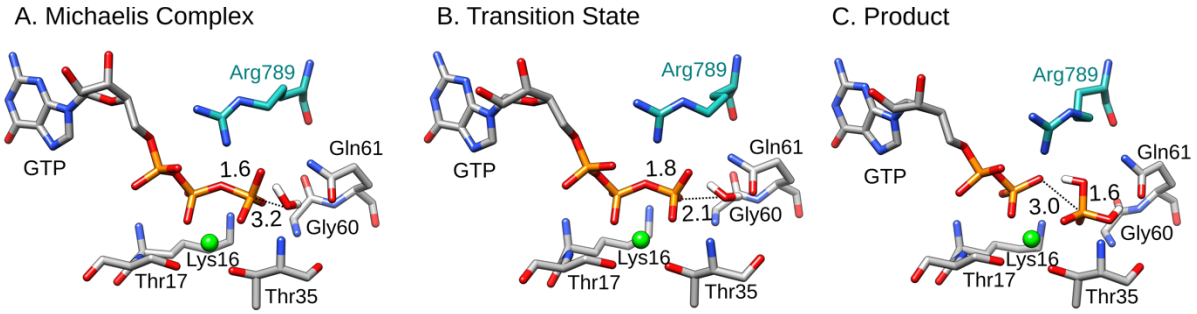

Figure S11. Structures of key stationary points, extracted from our empirical valence bond simulations of the RasGAP-catalyzed substrate-assisted hydrolysis of GTP. Shown here are (**A**) the Michaelis complex, (**B**) the transition state for the phosphoryl transfer reaction, and (**C**) the product complex. The P-O distances annotated on this figure (in Å) are average distances over all replicas, as presented in **Table S7**, and the structures shown in this figure were selected because they have P-O distances that are very similar to the average distances across all the EVB trajectories. The corresponding free energies for this reaction can be found in **Figure 3** and **Table S3**. Shown here are the substrate, nucleophilic water molecule, Mg^{2+} ion, and key catalytic residues. The remainder of the protein has been omitted for clarity.

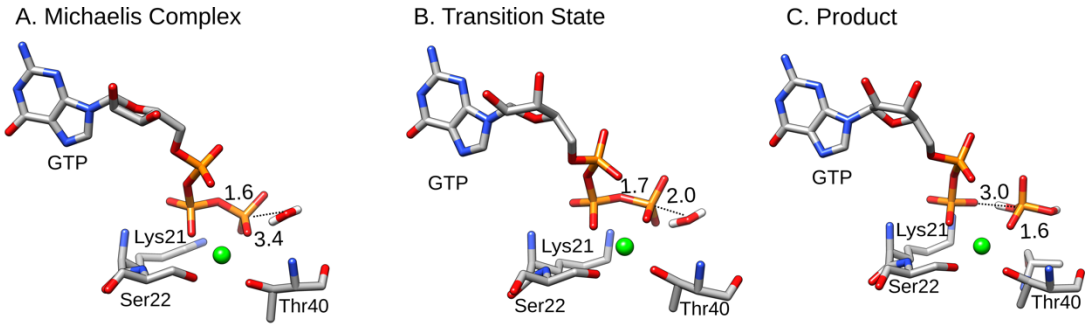

Figure S12. Structures of key stationary points, extracted from our empirical valence bond simulations of the Rab-catalyzed substrate-assisted hydrolysis of GTP. Shown here are (**A**) the Michaelis complex, (**B**) the transition state for the phosphoryl transfer reaction, and (**C**) the product complex. The P-O distances annotated on this figure (in Å) are average distances over all replicas, as presented in **Table S7**, and the structures shown in this figure were selected because they have P-O distances that are very similar to the average distances across all the EVB trajectories. The corresponding free energies for this reaction can be found in **Figure 3** and **Table S3**. Shown here are the substrate, nucleophilic water molecule, Mg^{2+} ion, and key catalytic residues. The remainder of the protein has been omitted for clarity.

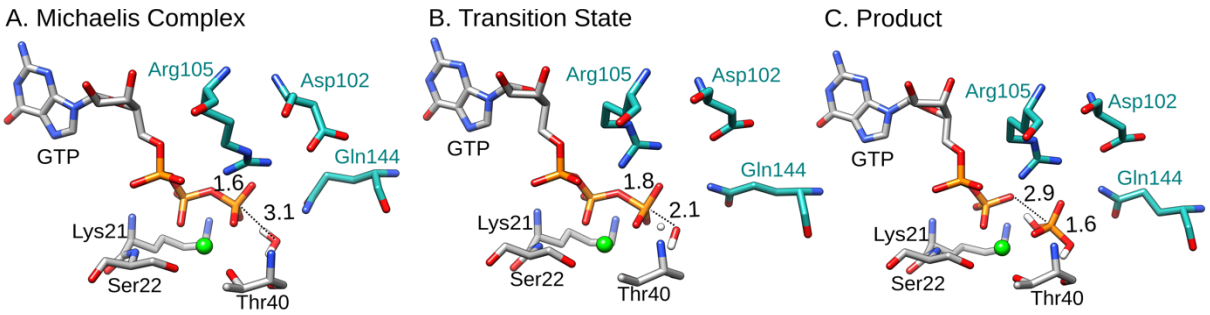

Figure S13. Structures of key stationary points, extracted from our empirical valence bond simulations of the RabGAP-catalyzed substrate-assisted hydrolysis of GTP. Shown here are (**A**) the Michaelis complex, (**B**) the transition state for the phosphoryl transfer reaction, and (**C**) the product complex. The P-O distances annotated on this figure (in Å) are average distances over all replicas, as presented in **Table S7**, and the structures shown in this figure were selected because they have P-O distances that are very similar to the average distances across all the EVB trajectories. The corresponding free energies for this reaction can be found in **Figure 3** and **Table S3**. Shown here are the substrate, nucleophilic water molecule, Mg^{2+} ion, and key catalytic residues. The remainder of the protein has been omitted for clarity.

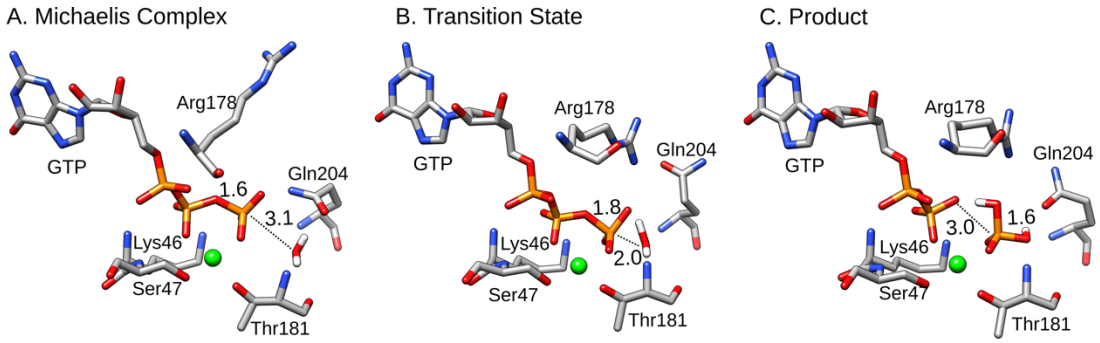

Figure S14. Structures of key stationary points, extracted from our empirical valence bond simulations of the $G_{\alpha i}$-catalyzed substrate-assisted hydrolysis of GTP. Shown here are (**A**) the Michaelis complex, (**B**) the transition state for the phosphoryl transfer reaction, and (**C**) the product complex. The P-O distances annotated on this figure (in Å) are average distances over all replicas, as presented in **Table S7**, and the structures shown in this figure were selected because they have P-O distances that are very similar to the average distances across all the EVB trajectories. The corresponding free energies for this reaction can be found in **Figure 3** and **Table S3**. Shown here are the substrate, nucleophilic water molecule, Mg^{2+} ion, and key catalytic residues. The remainder of the protein has been omitted for clarity.

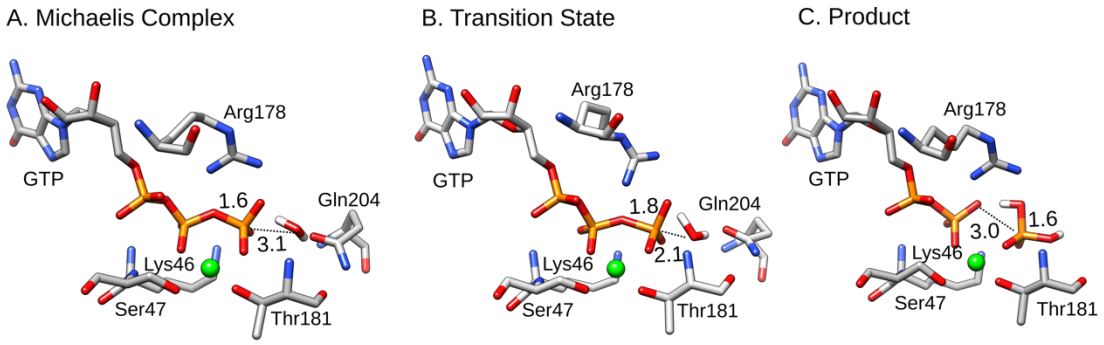

Figure S15. Structures of key stationary points, extracted from our empirical valence bond simulations of the $G_{\alpha i}$-RGS4-catalyzed substrate-assisted hydrolysis of GTP. Shown here are (**A**) the Michaelis complex, (**B**) the transition state for the phosphoryl transfer reaction, and (**C**) the product complex. The P-O distances annotated on this figure (in Å) are average distances over all replicas, as presented in **Table S7**, and the structures shown in this figure were selected because they have P-O distances that are very similar to the average distances across all the EVB trajectories. The corresponding free energies for this reaction can be found in **Figure 3** and **Table S3**. Shown here are the substrate, nucleophilic water molecule, Mg^{2+} ion, and key catalytic residues. The remainder of the protein has been omitted for clarity.

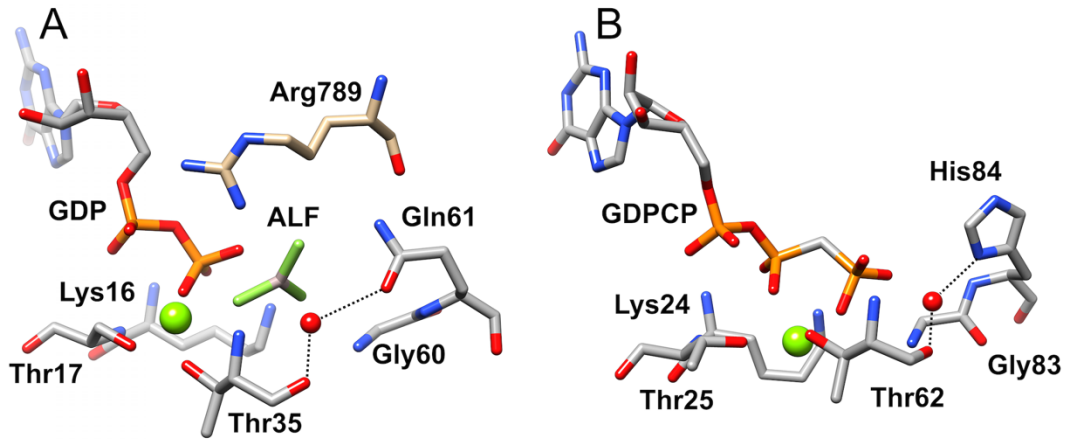

Figure S16. Comparison of the active sites of (**A**) the RasGAP complex (PDB ID: 1WQ1[3]) and (**B**) elongation factor thermounstable (EF-Tu) (PDB ID: 4V5L[4]), showing the active site residue, His84, present in EF-Tu in the same structural position as the residue Gln61 found in Ras and the RasGAP complex.

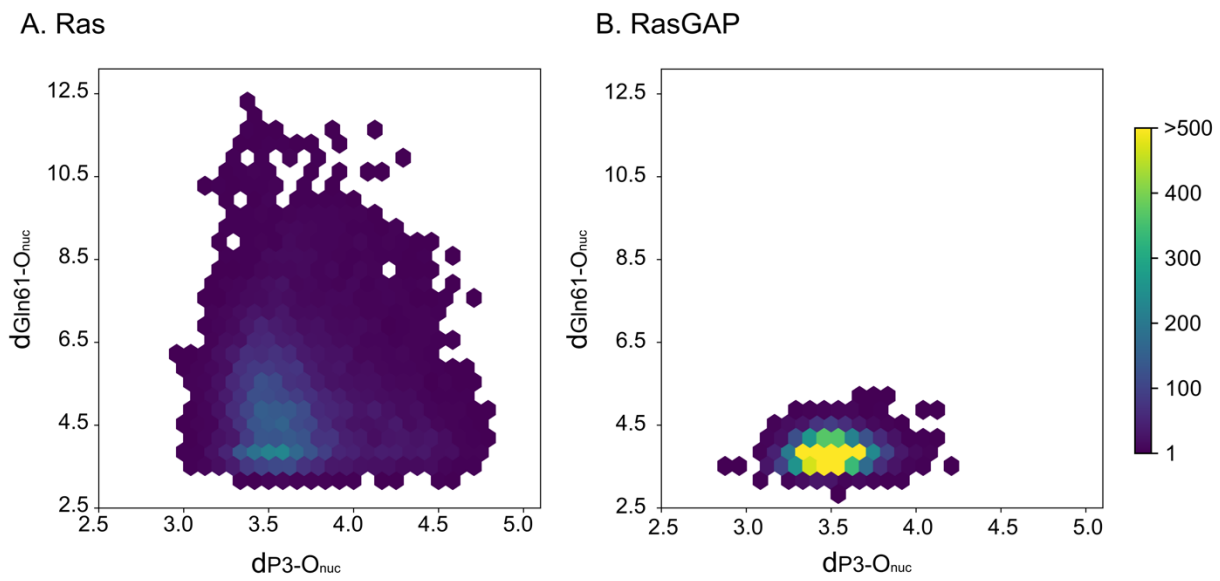

Figure S17. Conformational space of the nucleophilic water molecule sampled during 20 x 50ns (1 μs total) simulations of the Michaelis complexes of **(A)** Ras and **(B)** RasGAP, and defined as a function of the distance between the phosphorus atom of the γ-phosphate of the GTP (P3) and the oxygen atom of the nucleophilic water molecule (O_{nuc}, *x*-axis), and between the Cδ atom of the Gln61 side chain and the oxygen atom of the nucleophilic water molecule (O_{nuc}, *y*-axis). Simulations at the Michaelis complex were performed using the same protocol as for the equilibrations at the transition state, as described in the **Methodology** section, and using the same restraints as were applied in our EVB simulations (again, see the **Methodology** section). Snapshots were extracted for analysis every 100 ps.

S2. Supplementary Tables

Table S1. Overview of the different crystal structures used in this study, indicating the PDB ID, the resolution of the structure (in Å), any substrate or transition state analogues present in the structure (ligand) and any chemical modifications performed on the analogues, where present (modification).

PDB ID	Resolution (Å)	Ligand[a]	Modification[b]
1QRA[5]	1.6	GTP	-
1WQ1[3]	2.5	GDP; AF3	Al to P; F to O; bond between GDP and Al.
1GIA[6]	2.0	GSP	S to O
3NKV[7]	1.7	GNP	N to O
4HLQ[8]	3.3	GDP; BEF	Be to P; F to O; bond between GDP and Be.
621P[9]	2.4	GNP	N to O

[a] Here, the relevant ligands are guanosine-5´-triphosphate (GTP), guanosine-5´-diphosphate (GDP), 5´-guanosine-diphosphate-monothiophosphate (GSP), phophoaminophosphonic acid-guanylate ester (GNP), aluminum fluoride, AlF_3 (AF3), and beryllium fluoride, BeF_3^- (BEF). [b] All modifications were reverted to GTP, as described in the **Methodology** section.

Table S2. List of residues in their ionized states, as well as the protonation patterns of histidine residues, during the simulations.

Type	**Residue Number**[a]
Ras	
Asp	30, 33, 38, 54, 57, 69, 92, 119, 154
Glu	3, 31, 37, 62, 63, 76, 91, 98, 126, 143, 153, 162
Lys	5, 16, 42, 88, 101, 104, 117, 147
Arg	41, 68, 73, 97, 102, 123, 149
His-δ	94
His-ε	27, 166
RasGAP	
Asp	30, 33, 38, 54, 57, 69, 92, 119, 154, 748*, 775*, 782*, 972*
Glu	3, 31, 37, 62, 63, 76, 91, 98, 126, 143, 153, 162, 777*, 781*, 783*, 799*, 829*, 945*, 950*, 954*
Lys	5, 16, 42, 88, 101, 104, 117, 147, 803*, 834*, 884*, 935*, 949*, 961*, 964*
Arg	41, 68, 73, 97, 102, 123, 149, 749*, 776*, 789*, 892*, 894*, 903*, 913*, 928*
His-δ	94, 736*, 762*, 965*, 1005*
His-ε	27, 166, 743*, 811*, 812*, 847*, 883*, 986*, 999*, 1021*
Rab1	
Asp	16, 30, 31, 44, 63, 89, 92, 107, 124
Glu	35, 68, 94, 105, 149, 159
Lys	10, 21, 46, 100, 116, 122, 128, 129, 153
Arg	27, 48, 69, 71, 108
His-δ	-
His-ε	82
RabGAP	
Asp	16, 30, 31, 44, 63, 89, 92, 107, 124, 95*, 102*, 128*, 148*, 179*, 183*
Glu	35, 68, 94, 105, 149, 159, 116*, 120*, 124*
Lys	10, 21, 46, 100, 116, 122, 128, 129, 153, 94*, 186*

Arg	27, 48, 69, 71, 108, 90*, 104*, 105*, 108*, 109*, 119*
His-δ	141*, 187*, 227*, 277*
His-ε	82, 37*, 147*, 172*, 173*, 204*, 234*, 246*, 276*
$G_{\alpha i}$	
Asp	150, 158, 173, 200, 229, 231, 237, 251, 272, 328
Glu	43, 58, 65, 115, 116, 145, 186, 207, 216, 236, 238, 239, 245, 275, 276, 308
Lys	35, 46, 51, 54, 70, 180, 197, 209, 210, 248, 270, 271, 277, 280, 312, 317
Arg	86, 90, 142, 144, 161, 176, 178, 205, 208, 242
His-δ	213, 322
His-ε	57, 188, 195, 244
$G_{\alpha i}$-RGS4	
Asp	150, 158, 173, 200, 229, 231, 237, 251, 272, 328, 90*, 130*, 150*, 163*
Glu	43, 58, 65, 116, 145, 186, 207, 216, 236, 238, 239, 245, 275, 276, 297, 308, 61*, 83*, 86*, 87*, 117*, 126*, 135*, 136*, 151*, 161*
Lys	35, 46, 51, 54, 180, 197, 209, 210, 248, 270, 271, 277, 280, 317, 77*, 81*, 125*, 154*, 155*, 162*, 170*
Arg	86, 90, 142, 144, 161, 176, 178, 205, 208, 242, 134*, 139*, 166*, 167*
His-δ	213, 322, 69*
His-ε	57, 188, 195, 244

[a] Residues denoted with a star come from the GAP/RGS proteins. All residues not included in this table were kept in their unionized forms as they were outside the simulation sphere (see the **Methodology** section for further details).

Table S3. A comparison of calculated and experimental rates and activation free energies for the hydrolysis of GTP by a range of GTPases.[a]

System	k_{cat} (s^{-1})[b]	T_{exp} (K)[b]	$\Delta G^{\ddagger}_{exp}$	Solvent-Assisted		Substrate-Assisted	
				$\Delta G^{\ddagger}_{calc}$	ΔG^{0}_{calc}	$\Delta G^{\ddagger}_{calc}$	ΔG^{0}_{calc}
Water	--	298.15	27.9	27.9± 0.3	19.0 ± 0.5	37.2 ± 0.3	-7.4 ± 0.9
Ras	4.7 x 10^{-4}	310.15	22.9	23.9 ± 0.3	17.7 ± 0.5	30.8 ± 0.2	-13.8 ± 0.7
RasGAP	19.1	298.15	15.7	14.9 ± 0.4	7.8 ± 0.5	28.7 ± 0.3	-13.5 ± 0.6
Ras-Q61H	3.2 x 10^{-5}	310.15	24.6	24.8 ± 0.5	18.9 ± 0.6	31.7± 0.4	-11.4 ± 0.9
Rab	1.5 x 10^{-5}	293.15	23.6	24.0 ± 0.4	21.9 ± 0.4	36.9± 0.7	2.1± 0.8
RabGAP	0.9	268	17.2	14.0 ± 0.5	4.5 ± 0.8	23.6 ± 0.5	-19.7 ± 0.8
$G_{\alpha i}$	0.028	293.15	19.2	21.1 ± 0.5	15.8 ± 0.6	29.4 ± 0.3	-14.2 ± 0.7
$G_{\alpha i}$-RGS4	5.0	293.15[b]	16.2	16.5 ± 0.6	9.8 ± 0.7	29.6 ± 0.3	-14.4 ± 0.5

[a] $\Delta G^{\ddagger}_{exp}$ and $\Delta G^{\ddagger}_{calc}$ denote experimental and calculated activation free energies, respectively, and ΔG^{0}_{calc} denotes the calculated reaction free energies. All energies are shown in kcal mol^{-1}, and the calculated values are averages and standard error of the mean (s.e.m.) over 20 individual trajectories for each system, obtained as described in the **Methodology** section. The experimental values were derived from the corresponding experimentally measured k_{cat} (s^{-1}) using transition state theory. [b] The experimental k_{cat} values were obtained from ref. [10] for Ras and RasGAP, ref. [9] for Ras-Q61H, ref. [11] for $G_{\alpha i}$ and $G_{\alpha i}$-RGS4, and ref. [8] for Rab and RabGAP. T_{exp} denotes the temperature (in K) used in the experiment for the measurements. All simulations were performed at 300K. The activation free energy for the non-enzymatic reaction in water was taken from ref. [12]. As the experiments were performed at different temperatures, the corresponding temperatures used in the experiments are also provided in this table. All simulations were performed at 300 K. Finally, the EVB simulations for the non-enzymatic hydrolysis of GTP *via* a solvent-assisted pathway were calibrated to the experimental value, and the differences between the substrate- and solvent-assisted pathways in the non-enzymatic reaction were taken from our previous quantum chemical study,[13] as described in the **Methodology** section.

Table S4. Calculated activation and reaction free energies for the tautomerization step shown in **Figure S3**, during the non-enzymatic, Ras-catalyzed, and RasGAP-catalyzed hydrolyses of GTP.[a]

	$\Delta G^{\ddagger}_{calc}$	ΔG^{0}_{calc}
Water	4.0 ± 0.3	-26.4 ±0.6
Ras	3.3 ± 0.3	-30.2 ± 0.6
RasGAP	4.7 ± 0.3	-23.8 ± 0.6

[a] $\Delta G^{\ddagger}_{calc}$ and ΔG^{0}_{calc} denote the calculated activation and reaction free energies, respectively. All energies are shown in kcal mol^{-1}, and the calculated values are averages and standard error of the mean (s.e.m.) over 20 individual trajectories for each system, obtained as described in the **Methodology** section. In **Figure 3** of the main text, these values have been added to the energy of the intermediate (ΔG^{0}_{calc}) obtained from the preceding phosphoryl transfer step (**Table S3**) in order to obtain the full corrected free energy profile for these reactions.

Table S5. Average calculated phosphorus-oxygen distances to the departing leaving group ($P\text{-}O_{lg}$) and to the incoming nucleophile ($P\text{-}O_{nuc}$) at the reactant complexes and transition states for non-enzymatic GTP hydrolysis *via* solvent- and substrate-assisted mechanisms.[a]

	Solvent-Assisted	**Substrate-Assisted**
Michaelis Complex		
$P\text{-}O_{lg}$	1.71 ± 0.01	1.63 ± 0.00
$P\text{-}O_{nuc}$	4.03 ± 0.02	3.32 ± 0.01
O_{nuc} - O_{lg}	5.72 ± 0.02	4.80 ± 0.01
(First) Transition State		
$P\text{-}O_{lg}$	2.56 ± 0.01	1.82 ± 0.01
$P\text{-}O_{nuc}$	2.26 ± 0.01	2.05 ± 0.01
O_{nuc} - O_{lg}	4.82 ± 0.01	3.84 ± 0.01
Intermediate/Product		
$P\text{-}O_{lg}$	3.90 ± 0.02	3.42 ± 0.02
$P\text{-}O_{nuc}$	1.88 ± 0.01	1.58 ± 0.00
O_{nuc} - O_{lg}	5.76 ± 0.02	4.69 ± 0.03

[a] All values are averages and standard error of the mean over 400 individual snapshots, extracted from 20 independent empirical valence bond simulations, obtained as described in the **Methodology** section.

Table S6. Average calculated phosphorus-oxygen distances to the departing leaving group ($P\text{-}O_{lg}$) and to the incoming nucleophile ($P\text{-}O_{nuc}$) for the tautomerization step at the transition states and product states for non-enzymatic (water) as well as Ras- and RasGAP-catalyzed GTP hydrolysis.[a]

	Water	**Ras**	**RasGAP**
Second Transition State			
$P\text{-}O_{lg}$	3.81± 0.02	3.33 ± 0.02	3.31 ± 0.01
$P\text{-}O_{nuc}$	1.87 ± 0.00	1.87 ± 0.00	1.86. ± 0.00
O_{nuc} - O_{lg}	5.08 ± 0.06	5.17 ± 0.02	4.92 ± 0.01
Product			
$P\text{-}O_{lg}$	3.50 ± 0.02	3.22 ± 0.02	3.19 ± 0.01
$P\text{-}O_{nuc}$	1.65 ± 0.00	1.65 ± 0.00	1.64 ± 0.00
O_{nuc} - O_{lg}	4.60 ± 0.05	4.74 ± 0.01	4.70 ± 0.01

[a] All values are averages and standard error of the mean over 400 individual snapshots, extracted from 20 independent empirical valence bond simulations, obtained as described in the **Methodology** section.

Table S7. Average calculated phosphorus-oxygen distances to the departing leaving group ($P\text{-}O_{lg}$) and to the incoming nucleophile ($P\text{-}O_{nuc}$) at the Michaelis complexes, transition states and products for GTPase-catalyzed GTP hydrolysis *via* a substrate-assisted pathway.[a]

	Ras	**RasGAP**	**Ras Q61H**	**Rab**	**RabGAP**	**$G_{\alpha i}$**	**$G_{\alpha i}$-RGS4**
Michaelis Complex							
$P\text{-}O_{lg}$	1.63 ± 0.00	1.64 ± 0.00	1.63 ± 0.00	1.62 ± 0.00	1.62 ± 0.00	1.63 ± 0.00	1.62 ± 0.00
$P\text{-}O_{nuc}$	3.22 ± 0.01	3.21 ± 0.01	3.30 ± 0.01	3.45 ± 0.01	3.07 ± 0.01	3.14 ± 0.01	3.12 ± 0.01
O_{nuc} - O_{lg}	4.73 ± 0.01	4.68 ± 0.01	4.80 ± 0.01	3.62 ± 0.03	4.61 ± 0.01	4.66 ± 0.01	4.58 ± 0.01
Transition State							
$P\text{-}O_{lg}$	1.84 ± 0.01	1.85 ± 0.01	1.84 ± 0.01	1.75 ± 0.01	1.80 ± 0.01	1.85 ± 0.01	1.84 ± 0.01
$P\text{-}O_{nuc}$	2.04 ± 0.01	2.10 ± 0.01	2.05 ± 0.01	2.01 ± 0.01	2.12 ± 0.01	2.05 ± 0.01	2.08 ± 0.01
O_{nuc} - O_{lg}	3.85 ± 0.01	3.92 ± 0.01	3.86 ± 0.01	3.74 ± 0.01	3.90 ± 0.01	3.88 ± 0.01	3.89 ± 0.01
Product							
$P\text{-}O_{lg}$	2.97 ± 0.01	3.02 ± 0.01	2.98 ± 0.01	2.96 ± 0.01	2.93 ± 0.01	3.02 ± 0.01	2.98 ± 0.01
$P\text{-}O_{nuc}$	1.58 ± 0.00	1.58 ± 0.00	1.58 ± 0.00	1.57 ± 0.00	1.58 ± 0.00	1.58 ± 0.00	1.58 ± 0.00
O_{nuc} - O_{lg}	4.45 ± 0.01	4.50 ± 0.01	4.47 ± 0.01	3.87 ± 0.01	4.44 ± 0.01	4.52 ± 0.01	4.46 ± 0.01

[a] All values are averages and standard error of the mean over 400 individual snapshots, extracted from 20 independent empirical valence bond simulations, obtained as described in the **Methodology** section. For the corresponding values for the non-enzymatic reaction in aqueous solution, as well as the GTPase-catalyzed reaction proceeding through a solvent-assisted mechanism, see **Tables S5** and **Table 1** of the main text.

Table S8. Average distances between the Arg finger provided by the GAP (or the instrinc Arg, in the case of $G_{\alpha i}$) and the leaving group oxygen (O_{lg}) at the Michaelis complexes, transition states and products for GTPase-catalyzed substrate-assisted GTP hydrolysis.[a]

	RasGAP	**RabGAP**	**$G_{\alpha i}$**	**$G_{\alpha i}$-RGS4**
Michaelis Complex				
Arg:H_{ε}-O_{lg}	5.97 ± 0.02	6.06 ± 0.02	5.28 ± 0.09	5.54 ± 0.02
Arg:$H_{\eta 11}$-O_{lg}	**2.72 ± 0.01**	3.26 ± 0.02	7.63 ± 0.08	**2.21 ± 0.01**
Arg:$H_{\eta 12}$-O_{lg}	2.89 ± 0.01	**2.26 ± 0.02**	7.68 ± 0.07	3.20 ± 0.01
Arg:$H_{\eta 21}$-O_{lg}	4.78 ± 0.03	5.24 ± 0.02	**5.16 ± 0.12**	4.78 ± 0.02
Arg:$H_{\eta 22}$-O_{lg}	5.88 ± 0.02	3.64 ± 0.02	6.30 ± 0.11	3.31 ± 0.01
Transition State				
Arg:H_{ε}-O_{lg}	6.03 ± 0.02	6.01 ± 0.02	5.34 ± 0.10	5.64 ± 0.02
Arg:$H_{\eta 11}$-O_{lg}	**2.76 ± 0.01**	3.28 ± 0.01	7.50 ± 0.09	**1.98 ± 0.01**
Arg:$H_{\eta 12}$-O_{lg}	3.01 ± 0.02	**2.11 ± 0.01**	7.56 ± 0.07	3.26 ± 0.01
Arg:$H_{\eta 21}$-O_{lg}	4.93 ± 0.03	5.14 ± 0.03	**5.14 ± 0.13**	4.76 ± 0.01
Arg:$H_{\eta 22}$-O_{lg}	6.00 ± 0.02	3.52 ± 0.02	6.20 ± 0.12	3.25 ± 0.01
Product				
Arg:H_{ε}-O_{lg}	5.57 ± 0.02	5.70 ± 0.02	**5.48 ± 0.09**	5.47 ± 0.01
Arg:$H_{\eta 11}$-O_{lg}	**2.49 ± 0.01**	3.10 ± 0.01	7.37 ± 0.09	**1.66 ± 0.01**
Arg:$H_{\eta 12}$-O_{lg}	2.90 ± 0.02	**1.74 ± 0.01**	7.36 ± 0.08	3.14 ± 0.01
Arg:$H_{\eta 21}$-O_{lg}	4.74 ± 0.03	4.87 ± 0.02	**5.49 ± 0.12**	4.53 ± 0.01
Arg:$H_{\eta 22}$-O_{lg}	5.66 ± 0.02	2.36 ± 0.01	6.37 ± 0.12	3.07 ± 0.01

[a] H_{ε} is the hydrogen at the N_{ε} nitrogen atom of Arg. $H_{\eta 11}$, $H_{\eta 12}$ and $H_{\eta 21}$, $H_{\eta 22}$ are the hydrogen atoms at $N_{\eta 1}$ and $N_{\eta 2}$ nitrogens of Arg, respectively. All values are averages and standard error of the mean over 400 individual snapshots, extracted from 20 independent empirical valence bond simulations, obtained as described in the **Methodology** section. The corresponding values for the solvent-assisted mechanism can be found in **Table 2** of the main text. The closest interactions, in each case, are highlighted in bold.

Table S9. Calculated activation and reaction free energies for Ras-catalyzed GTP hydrolysis *via* solvent and substrate assisted pathways, with and without a 10 kcal mol^{-1} $Å^{-2}$ harmonic positional restraint placed on the Gln61 side chain.[a]

	$\Delta G^{\ddagger}_{calc}$	ΔG^{0}_{calc}
Solvent-assisted pathway		
Flexible Gln61	23.9 ± 0.3	17.7 ± 0.5
Restrained Gln61	17.6 ± 0.5	11.2 ± 0.5
Substrate-assisted pathway		
Flexible Gln61	30.8 ± 0.2	-13.8 ± 0.7
Restrained Gln61	29.6 ± 0.3	-13.8 ± 1.1

[a] $\Delta G^{\ddagger}_{calc}$ and ΔG^{0}_{calc} denote the calculated activation and reaction free energies, respectively. All energies are shown in kcal mol^{-1}, and the calculated values are averages and standard error of the mean (s.e.m.) over 20 individual trajectories for each system, obtained as described in the **Methodology** section.

Table S10. Loss of conformational entropy of the catalytic glutamine residue upon protein folding of different GTPases considered in this work, calculated using the Predicting Loss of Protein S(entropy) (PLOPS)[14] webserver.[a]

System	Residue	TΔS Backbone	TΔS Sidechain	TΔS Total
Ras	Q61	1.15	0.39	1.54
RasGAP	Q61	1.15	1.00	2.15
Rab	Q67	1.15	0.44	1.59
RabGAP	Q144	1.15	0.99	2.14
$G_{\alpha i}$	Q204	1.15	0.75	1.90
$G_{\alpha i}$-RGS4	Q204	1.15	0.96	2.11

[a] All values are presented in kcal mol^{-1}. Note that as PLOPS calculates entropy *loss* upon protein folding, a more positive TΔS value in this table indicates that the side chain is more ordered in the folded state of the protein. The PLOPS webserver can be accessed at https://godzilla.uchicago.edu/pages/PLOPS/live/index.html.

Table S11. Metal-ligand distances in the initial crystal structures and during our simulations of solvent- and substrate-assisted GTP hydrolysis catalyzed by different GTPases.[a]

	Ras	**RasGAP**	**Ras Q61H**	**Rab**	**RabGAP**	**$G_{\alpha i}$**	**$G_{\alpha i}$-RGS4**
Initial crystal structures							
Ser:OG [b]	2.16	2.09	2.09	2.17	2.19	2.13	2.13
Thr:OG1 [b]	2.18	2.16	2.21	2.20	2.15	2.12	2.13
GTP:O- [b]	2.12	2.06	2.11	2.10	2.10	2.04	2.05
GTP:Ob [b]	2.11	2.07	2.10	2.03	2.08	2.06	2.16
HOH 1 [b]	2.09	2.11	2.19	2.15	2.14	2.14	2.09
HOH 2 [b]	2.16	2.12	2.11	2.14	2.13	2.10	2.17
Solvent-assisted pathway							
Ser:OG [b]	2.15 ± 0.05	2.14 ± 0.05	2.14 ± 0.05	2.14 ± 0.01	2.15 ± 0.01	2.15 ± 0.05	2.14 ± 0.04
Thr:OG1 [b]	2.17 ± 0.05	2.16 ± 0.05	2.16 ± 0.05	2.16 ± 0.01	2.17 ± 0.01	2.17 ± 0.05	2.15 ± 0.05
GTP:O- [b]	2.08 ± 0.04	2.08 ± 0.04	2.08 ± 0.04	2.10 ± 0.00	2.10 ± 0.00	2.08 ± 0.04	2.08 ± 0.04
GTP:Ob [b]	2.11 ± 0.04	2.10 ± 0.04	2.10 ± 0.04	2.08 ± 0.00	2.08 ± 0.00	2.11 ± 0.04	2.11 ± 0.04
HOH 1 [b]	2.13 ± 0.05	2.12 ± 0.04	2.13 ± 0.05	2.13 ± 0.00	2.14 ± 0.00	2.12 ± 0.05	2.12 ± 0.04
HOH 2 [b]	2.12 ± 0.05	2.13 ± 0.05	2.13 ± 0.05	2.12 ± 0.00	2.13 ± 0.00	2.13 ± 0.05	2.13 ± 0.05
Substrate-assisted pathway							
Ser:OG [b]	2.14 ± 0.05	2.13 ± 0.05	2.14 ± 0.05	2.12 ± 0.00	2.14 ± 0.01	2.15 ± 0.05	2.14 ± 0.05
Thr:OG1 [b]	2.16 ± 0.05	2.15 ± 0.05	2.16 ± 0.05	2.13 ± 0.00	2.16 ± 0.01	2.16 ± 0.05	2.15 ± 0.05
GTP:O- [b]	2.08 ± 0.04	2.06 ± 0.04	2.08 ± 0.04	2.11 ± 0.00	2.10 ± 0.00	2.08 ± 0.04	2.06 ± 0.04
GTP:Ob [b]	2.11 ± 0.04	2.11 ± 0.04	2.11 ± 0.04	2.07 ± 0.00	2.07 ± 0.00	2.11 ± 0.04	2.11 ± 0.04
HOH 1 [b]	2.13 ± 0.05	2.12 ± 0.04	2.13 ± 0.05	2.14 ± 0.00	2.14 ± 0.00	2.12 ± 0.05	2.12 ± 0.04
HOH 2 [b]	2.12 ± 0.05	2.13 ± 0.05	2.13 ± 0.05	2.16 ± 0.01	2.14 ± 0.00	2.13 ± 0.05	2.14 ± 0.05

[a] Values for both solvent- and substrate-assisted mechanism are averages and standard error of the mean over 10 000 individual snapshots, extracted every 100ps from the 20x50ns independent simulations (1μs total), obtained as described in the **Methodology** section. Values for the initial structure were obtained from the corresponding PDB structures used for our simulations, specifically, 1QRA[5, 15] (Ras), 1WQ1[3, 15] (RasGAP), 1GIA[6, 15] ($G_{\alpha i}$-subunit), 3NKV[7, 15] (Rab), chains I and J from 4HLQ[8, 15] (Rab1GAP), 621P[9, 15] (Ras Q61H variant). In the case of the $G_{\alpha i}$-RGS4 complex, a refined crystal structure was used as a starting point for the simulations.[16] [b] In all systems, the octahedral coordination sphere of Mg^{2+} is formed by two oxygen atoms belonging to the side chain residues of the

GTPase, namely a Ser and a Thr, two oxygens of the GTP triphosphate moiety (where Ob denotes the oxygen bridging the β,γ-phosphate and O^- denotes a non-bridging oxygen from the β-phosphate) and the oxygen atoms of two water molecules. The relevant sidechains in each system are the side chains of Ser17 and Thr35 in wild-type and Q61H mutant Ras and RasGAP, the side chains of Ser22 and Thr40 in Rab and RabGAP, the side chains of Ser14 and Thr148 in $G_{\alpha i}$, and the side chains of Ser47 and Thr181 in $G_{\alpha i}$-RGS4.

Table S12. Average number of water molecules found within 6Å of phosphorus atom of the γ-phosphate group of GTP (upper section), and the average number of hydrogen bonds formed between key species, as annotated, at the Michaelis complexes, transition states and intermediates of solvent-assisted GTPase-catalyzed GTP hydrolysis.[a]

	Ras	**RasGAP**	**Rab**	**RabGAP**	**$G_{\alpha i}$**	**$G_{\alpha i}$-RGS4**
Average number of water molecules within 6Å of the phosphorus atom of the γ-phosphate of GTP[b]						
Michaelis Complex	8.28 ± 0.08	2.05 ± 0.01	7.02 ± 0.08	2.76 ± 0.05	4.90 ± 0.06	3.46 ± 0.06
First Transition State	8.26 ± 0.09	2.00 ± 0.00	6.42 ± 0.07	2.86 ± 0.05	5.25 ± 0.07	3.22 ± 0.05
Intermediate	8.94 ± 0.09	2.00 ± 0.00	6.13 ± 0.07	3.05 ± 0.05	5.30 ± 0.08	3.39 ± 0.05
Average number of hydrogen bonds formed between the γ-phosphate and the solvent molecules[b]						
Michaelis Complex	2.76 ± 0.06	0.04± 0.01	1.59 ± 0.05	0.14 ± 0.02	0.85 ± 0.04	0.61 ± 0.04
First Transition State	2.01 ± 0.04	-	1.50 ± 0.03	0.18 ± 0.01	0.53 ± 0.03	0.14 ± 0.02
Intermediate	1.87 ± 0.04	-	1.29 ± 0.03	0.17 ± 0.03	0.29 ± 0.03	0.17 ± 0.02
Average number of hydrogen bonds formed between the γ-phosphate and the GTPase						
Michaelis Complex	1.60 ± 0.04	2.65 ± 0.04	2.76 ± 0.04	3.34 ± 0.04	2.98 ± 0.04	2.88 ± 0.04
First Transition State	2.01 ± 0.04	3.64 ± 0.04	3.33 ± 0.05	3.75 ± 0.04	3.20 ± 0.04	3.53 ± 0.03
Intermediate	2.11 ± 0.04	3.78 ± 0.02	3.45 ± 0.05	4.03 ± 0.03	3.37 ± 0.04	3.79 ± 0.04
Average number of hydrogen bonds formed between the carbonyl oxygen of the active site Gln and the nucleophilic water molecule						
Michaelis Complex	0.16 ± 0.02	0.74 ± 0.02	-	0.60 ± 0.04	0.63 ± 0.03	0.39 ± 0.02
First Transition State	0.25 ± 0.02	0.84 ± 0.02	0.71 ± 0.02	0.91 ± 0.03	0.83 ± 0.02	0.77 ± 0.02
Intermediate	0.31 ± 0.02	0.90 ± 0.01	0.80 ± 0.02	0.90 ± 0.03	0.88 ± 0.02	0.75 ± 0.02

[a] All values are averages and standard error of the mean over 400 individual snapshots, extracted from 20 independent empirical valence bond simulations, obtained as described in the **Methodology** section. The corresponding values for the substrate-assisted mechanism can be found in **Table S13**. [b] The nucleophilic water molecule is excluded from these numbers. Note that "-" in this table indicates that no hydrogen bonds were found for this system.

Table S13. Average number of water molecules found within 6Å of phosphorus atom of the γ-phosphate group of GTP (upper section), and the average number of hydrogen bonds formed between key species, as annotated, at the Michaelis complexes, transition states and products of substrate-assisted GTPase-catalyzed GTP hydrolysis.[a]

	Ras	**RasGAP**	**Rab**	**RabGAP**	**$G_{\alpha i}$**	**$G_{\alpha i}$-RGS4**
Average number of water molecules within 6Å of the phosphorus atom of the γ-phosphate of GTP[b]						
Michaelis Complex	8.22 ± 0.08	2.21 ± 0.02	6.53 ± 0.07	3.12 ± 0.05	5.46 ± 0.07	3.62 ± 0.04
Transition State	7.61 ± 0.09	2.18 ± 0.02	6.24 ± 0.07	2.77 ± 0.04	4.86 ± 0.06	3.22 ± 0.03
Product	7.67 ± 0.08	2.30 ± 0.03	8.50 ± 0.11	2.96 ± 0.05	5.33± 0.07	3.20 ± 0.04
Average number of hydrogen bonds formed between the γ-phosphate and the solvent molecules[b]						
Michaelis Complex	2.32 ± 0.04	0.07 ± 0.01	1.40 ± 0.04	0.22 ± 0.02	1.06 ± 0.05	0.85 ± 0.02
Transition State	1.41 ± 0.04	0.04 ± 0.01	1.25 ± 0.03	0.12 ± 0.02	0.37 ± 0.03	0.50 ± 0.02
Product	0.81 ± 0.03	0.07 ± 0.01	1.85 ± 0.06	0.05 ± 0.01	0.25 ± 0.02	0.17 ± 0.02
Average number of hydrogen bonds formed between the γ-phosphate and the GTPase						
Michaelis Complex	1.62 ± 0.03	2.77 ± 0.04	2.83 ± 0.05	3.25 ± 0.04	2.45 ± 0.04	2.24 ± 0.03
Transition State	1.95 ± 0.03	2.79 ± 0.03	2.74 ± 0.05	3.17 ± 0.04	2.63 ± 0.04	2.48 ± 0.03
Product	2.21 ± 0.03	2.60 ± 0.04	1.36 ± 0.05	3.68 ± 0.03	2.64 ± 0.04	2.66 ± 0.03
Average number of hydrogen bonds formed between the carbonyl oxygen of the active site Gln and the nucleophilic water molecule						
Michaelis Complex	-	0.45 ± 0.02	-	0.44 ± 0.04	0.09 ± 0.01	0.27 ± 0.02
Transition State	0.02 ± 0.01	0.56 ± 0.02	0.08 ± 0.01	0.51 ± 0.03	0.01 ± 0.00	0.41 ± 0.02
Product	0.04 ± 0.01	0.66 ± 0.02	0.31 ± 0.02	0.52 ± 0.03	0.10 ± 0.01	0.80 ± 0.02

[a] All values are averages and standard error of the mean over 400 individual snapshots, extracted from 20 independent empirical valence bond simulations, obtained as described in the **Methodology** section. The corresponding values for the solvent-assisted mechanism can be found in **Table S12**. [b] The nucleophilic water molecule is excluded from these numbers. Note that "-" in this table indicates that no hydrogen bonds were found for this system.

S3. Empirical Valence Bond Parameters

Table S14. EVB off-diagonal element (H_{ij}) and gas phase shift (α_i) parameters, calibrated as described in the main text.

Mechanism	Reaction	H_{ij} (kcal mol^{-1})	α_i (kcal mol^{-1})
Solvent-assisted	Phosphate Hydrolysis	77.36	262.42
Solvent-assisted	Tautomerization	25.70	-197.35
Substrate -assisted	GTP hydrolysis	50.94	46.69

Table S15. List of the atom types and van der Waals parameters used to describe atoms constituting the reacting part of the system.

Type	A_i (kcal$^{1/2}$ mol$^{1/2}$ Å^6)	B_i (kcal$^{1/2}$ mol$^{1/2}$ Å^3)	C_i (kcal mol^{-1})	α_i (Å^2)	$A_{1\text{-}4}$ (kcal$^{1/2}$ mol$^{1/2}$Å^3)	$B_{1\text{-}4}$ (kcal$^{1/2}$ mol$^{1/2}$ Å^3)	Mass (a.u.)
CT	944.52	22.03			667.88	15.58	12.01
HC	69.58	4.91			49.20	3.47	1.01
HO	0.01	0.04	5	2.5	0.00	0.03	1.01
HW	0.00	0.00	5	2.5	0.00	0.00	1.01
Olg	873.79	27.96	500	2.0	617.86	19.76	16.00
OH	401.02	17.32	53	2.5	283.56	12.25	16.00
OP1	873.79	27.96	53	2.5	617.86	19.76	16.00
OP2	626.39	23.67	53	2.5	442.92	16.74	16.00
OW	726.89	24.39	53	2.5	539.44	17.25	16.00
OW2	726.89	24.39	60	2.5	539.44	17.25	16.00
O1	445.13	18.25	150	2.0	314.76	12.91	16.00
O2	873.79	27.96	150	2.0	617.86	19.76	16.00
P1	2447.79	46.79	45	1.4	1730.85	33.09	30.97
P2	2447.79	46.79	40	1.5	1730.85	33.09	30.97
P3	2447.79	46.79	43	2.5	1730.85	33.09	30.97

[a] For all atoms except the reacting atoms, a standard 6-12 Lennard-Jones potential was used. In the case of the reacting atoms, which change bonding patterns between atoms *i* and *j*, an alternate function of the form $V_{react} = C_i C_j \exp(-\alpha_i \alpha_j r_{ij})$ was used to prevent artificial repulsion between these atoms as bonding patterns change. r_{ij} denotes the distance (Å) between atoms *i* and *j*. Note that this was only applied to atoms that change bonding patterns during the reaction, and not to all atoms in the system. For atom type assignment see **Table S16**.

Table S16. Atom types in the different VB states (**Figure S1** and **S2**) used to describe GTP hydrolysis *via* both solvent- and substrate-assisted mechanisms.[a]

Atom number	State 1_{solv}	State 2_{solv}	State 3_{solv}	State 1_{sub}	State 2_{sub}
1	HC	HC	HC	HC	HC
2	CT	CT	CT	CT	CT
3	HC	HC	HC	HC	HC
4	O1	O1	O1	O1	O1
5	P1	P1	P1	P1	P1
6	OP1	OP1	OP1	OP1	OP1
7	OP1	OP1	OP1	OP1	OP1
8	O1	O1	O1	O1	O1
9	P1	P1	P1	P1	P1
10	OP1	OP1	OP1	OP1	OP1
11	OP1	OP1	OP1	OP1	OP1
12	O1	Olg	Olg	O1	O2
13	P1	P2	P2	P3	P3
14	OP1	OP2	OH	OP1	OH
15	OP1	OP2	OP2	OP1	OP2
16	OP1	OP2	OP2	OP1	OP2
17	OW2	OH	OH	OW	OH
18	HW	HO	HO	HW	HO
19	HW	HO	HO	HW	HO

[a] See **Figure S1 and S2** for the atom numbering, **Table S15** for the corresponding van der Waals parameters and **Table S17** for the corresponding partial charges. The subscripts solv and sub denote solvent- and substrate-assisted mechanisms, respectively.

Table S17. Atomic partial charges in the different VB states (**Figure S1** and **S2**) used to describe GTP hydrolysis *via* both solvent- and substrate-assisted mechanisms.[a]

Atom number	State 1_{solv}	State 2_{solv}	State 3_{solv}	State 1_{sub}	State 2_{sub}
1	0.067907	0.067909	0.067909	0.067907	0.067909
2	0.055805	0.055807	0.055807	0.055805	0.055807
3	0.067907	0.067909	0.067909	0.067907	0.067909
4	-0.598641	-0.657813	-0.657813	-0.598641	-0.657813
5	1.253323	1.493096	1.493096	1.253323	1.493096
6	-0.879813	-0.947275	-0.947275	-0.879813	-0.947275
7	-0.879813	-0.947275	-0.947275	-0.879813	-0.947275
8	-0.568844	-0.634516	-0.634516	-0.568844	-0.634516
9	1.385334	1.367380	1.367380	1.385334	1.367380
10	-0.889312	-0.955074	-0.955074	-0.889312	-0.955074
11	-0.889312	-0.955074	-0.955074	-0.889312	-0.955074
12	-0.532148	-0.955074	-0.955074	-0.532148	-0.955074
13	1.265125	1.389070	1.565000	1.265125	1.565000
14	-0.952506	-0.861224	-0.692500	-0.952506	-0.692500
15	-0.952506	-0.861224	-0.970000	-0.952506	-0.970000
16	-0.952506	-0.861224	-0.970000	-0.952506	-0.970000
17	-0.834000	-0.647508	-0.692500	-0.834000	-0.692500
18	0.417000	0.421055	0.380000	0.417000	0.380000
21	0.417000	0.421055	0.380000	0.417000	0.380000

[a] For the corresponding atom numbering, see **Figure S1 and S2**, and for details of how these charges were derived, see the main text. The subscripts solv and sub denote solvent- and substrate-assisted mechanisms, respectively.

Table S18. Bond types and corresponding parameters for the covalent bonds of the reacting part of the system.[a]

Bond type	D (kcal mol^{-1})	α (Å^{-2})	r_0 (Å)	K_b (kcal mol^{-1} Å^{-2})	r_0 (Å)
0	Not Set				
1	60.0	1.5	1.610		
2	95.0	2.0	1.610		
3	95.0	1.5	1.880		
4	110.0	2.0	0.940		
5	245.8	1.5	0.957		
6	245.8	1.5	0.975		
7				460.0	1.660
8				460.0	1.670
9				460.0	1.690
10				460.0	1.967
11				717.0	1.600
12				717.0	1.610
13				1000.0	1.963
14				1104.8	0.975
15				1106.0	0.945
16				1106.0	0.957
17				1046.5	1.510
18				1050.0	1.480
19				1050.0	1.500
20				1050.0	1.540

[a] The bonds between non-reacting atoms are described using harmonic potentials, $V_{\text{harmonic}} = 0.5K_b\,(r_{ij} - r_0)^2$, while bonds between reacting atoms are described using Morse potentials $V_{\text{Morse}} = D\,\{1 - \exp[-\alpha\,(r_{ij} - r_0)]\}^2$. The bond-type assignments for the initial phosphoryl transfer reaction in the solvent-assisted mechanism, the subsequent tautomerization step, and for the substrate-assisted mechanism, are shown in **Tables S19 – S21**, respectively.

Table S19. Bond types used to describe the covalent bonds of the reacting part of the system, for the initial phosphoryl transfer step during solvent-assisted GTP hydrolysis (for the VB states see **Figure S1**).[a]

Atom number		**Bond type**	
#1	**#2**	**State 1**	**State 2**
12	13	1	0
13	17	0	3
8	9	8	7
4	5	9	8
5	8	11	12
9	10	19	20
9	11	19	20
9	12	11	20
13	14	20	17
13	15	20	17
13	16	20	17
17	18	16	14
17	19	16	14

[a] See **Figure S1** for the atom numbering.

Table S20. Bond types used to describe the covalent bonds of the reacting part of the system, for the tautomerization step during solvent-assisted GTP hydrolysis (for the VB states see **Figure S1**).[a]

Atom number		Bond type	
#1	**#2**	**State 2**	**State 3**
17	19	6	0
14	19	0	4
13	14	17	10
13	15	17	18
13	16	17	18
13	17	13	10
17	18	14	15
8	9	7	7
4	5	8	8
5	8	12	12
9	10	20	20
9	11	20	20
9	12	20	20

[a] See **Figure S1** for the atom numbering.

Table S21. Bond types used to describe the covalent bonds of the reacting part of the system, for GTP hydrolysis *via* a substrate-assisted mechanism, using the VB states described in **Figure S2**.[a]

Atom number		Bond type	
#1	**#2**	**State 1**	**State 2**
12	13	1	0
17	19	5	0
14	19	0	4
13	17	0	2
8	9	8	7
4	5	9	8
5	8	11	12
9	10	19	20
9	11	19	20
9	12	11	20
13	14	20	10
13	15	20	18
13	16	20	18
17	18	16	15

[a] See **Figure S2** for the atom numbering.

Table S22. Angle types and the corresponding parameters used for bending adjacent bonds in the reacting part of the system.[a]

Angle type	K_a (kcal mol^{-1} rad^{-2})	Θ (°)
0	Not Set	
1	47.80	110.50
2	90.00	102.60
3	90.00	108.50
4	97.70	112.07
5	99.52	105.88
6	155.20	98.09
7	163.52	118.05
8	239.00	98.50
9	200.00	104.52
10	200.00	108.23
11	280.00	119.90
12	280.00	122.50

[a] The angle potential is described using the potential $V_{angle} = 0.5\ \Sigma K_a(\Theta-\Theta_0)^2$. The angle-type assignments for the initial phosphoryl transfer reaction in the solvent-assisted mechanism, the subsequent tautomerization step, and for the substrate-assisted mechanism, are shown in **Tables S23 – S25**, respectively.

Table S23. Angle types used to describe the covalent bonds of the reacting part of the system, for the initial phosphoryl transfer step during solvent-assisted GTP hydrolysis (for the VB states see **Figure S1**).[a]

Atom number			Angle type	
#1	**#2**	**#3**	**State 1**	**State 2**
12	13	14	10	0
12	13	15	10	0
12	13	16	10	0
9	12	13	1	0
14	13	17	0	6
15	13	17	0	6
16	13	17	0	6
13	17	18	0	4
13	17	19	0	4
6	5	8	2	10
10	9	12	10	12
14	13	15	12	7
14	13	16	12	7
7	5	8	2	10
11	9	12	10	12
15	13	16	12	7
8	9	12	8	10
4	5	8	4	2
18	17	19	9	5

[a]See **Figure S1** for the atom numbering.

Table S24. Angle types used to describe the covalent bonds of the reacting part of the system, for the tautomerization step during solvent-assisted GTP hydrolysis (for the VB states see **Figure S1**).[a]

Atom number			Angle type	
#1	**#2**	**#3**	**State 2**	**State 3**
14	13	17	6	2
15	13	17	6	10
16	13	17	6	10
13	17	19	4	0
13	17	18	4	3
14	13	15	7	10
14	13	16	7	10
15	13	16	7	11
19	17	19	5	0
13	14	19	0	3
10	9	12	12	12
7	5	8	10	10
11	9	12	12	12
8	9	12	10	10
4	5	8	2	2

[a] See **Figure S1** for the atom numbering.

Table S25. Angle types used to describe the covalent bonds of the reacting part of the system, for GTP hydrolysis *via* a substrate-assisted mechanism, using the VB states described in **Figure S2**.[a]

Atom number			Angle type	
#1	**#2**	**#3**	**State 1**	**State 2**
12	13	14	10	0
12	13	15	10	0
12	13	16	10	0
9	12	13	1	0
18	17	19	9	0
14	13	17	0	2
15	13	17	0	10
16	13	17	0	10
13	14	19	0	3
13	17	18	0	3
6	5	8	2	10
10	9	12	10	12
14	13	15	12	10
14	13	16	12	10
7	5	8	2	10
11	9	12	10	12
15	13	16	12	11
8	9	12	8	10
4	5	8	8	2

[a] See **Figure S2** for the atom numbering.

Table S26. Torsion types and the corresponding parameters for rotation of dihedrals in the reacting part of the system.[a]

Torsion type	K_φ (kcal mol^{-1} rad^{-2})	n	φ_0 (°)
0	Not Set		
1	0.00000	1.0	0.0
2	0.02271	-5.0	0.0
3	0.19778	-4.0	180.0
4	0.45949	-3.0	0.0
5	-0.24857	-2.0	180.0
6	-2.26757	1.0	0.0
7	0.15476	-3.0	0.0
8	0.0006	1.0	0.0
9	-0.00224	-5.0	0.0
10	0.00209	-4.0	180.0
11	0.59826	-3.0	0.0
12	-0.08724	-2.0	180.0
13	1.35188	1.0	0.0
14	-0.09097	-5.0	0.0
15	0.15685	-4.0	180.0
16	0.58482	-3.0	0.0
17	-0.89627	-2.0	180.0
18	-0.35761	1.0	0.0
19	0.00762	-5.0	0.0
20	0.06603	-4.0	180.0
21	0.15341	-3.0	0.0
22	-0.08246	-2.0	180.0
23	-0.75615	1.0	0.0
24	0.01509	-5.0	0.0
25	0.13175	-4.0	180.0
26	0.30608	-3.0	0.0
27	-0.16611	-2.0	180.0
28	-1.51141	1.0	0.0

[a] The torsion angle potential is described using the potential $V_{torsion} = K_\varphi(1+\cos(n\varphi-\varphi_0))$. The torsion-type assignments for the initial phosphoryl transfer reaction in the solvent-assisted mechanism, the subsequent tautomerization step, and for the substrate-assisted mechanism, are shown in **Tables S27 – S29**, respectively.

Table S27. Torsion types used to describe the covalent bonds of the reacting part of the system, for the initial phosphoryl transfer step during solvent-assisted GTP hydrolysis (for the VB states see **Figure S1**).[a]

Atom number				Torsion type	
#1	**#2**	**#3**	**#4**	**State 1**	**State 2**
10	9	12	13	1	0
11	9	12	13	1	0
8	9	12	13	2	0
8	9	12	13	3	0
8	9	12	13	4	0
8	9	12	13	5	0
8	9	12	13	6	0
9	12	13	14	7	0
9	12	13	14	8	0
9	12	13	15	7	0
9	12	13	15	8	0
9	12	13	16	7	0
9	12	13	16	8	0
14	13	17	18	0	1
14	13	17	19	0	1
15	13	17	18	0	1
15	13	17	19	0	1
16	13	17	18	0	1
16	13	17	19	0	1
2	4	5	8	9	14
2	4	5	8	10	15
2	4	5	8	11	16
2	4	5	8	12	17
2	4	5	8	13	18
4	5	8	9	19	24
4	5	8	9	20	25
4	5	8	9	21	26
4	5	8	9	22	27
4	5	8	9	23	28
5	8	9	12	2	0
5	8	9	12	3	0
5	8	9	12	4	0
5	8	9	12	5	0
5	8	9	12	6	1

[a] See **Figure S1** for the atom numbering.

Table S28. Torsion types used to describe the covalent bonds of the reacting part of the system, for the tautomerization step during solvent-assisted GTP hydrolysis (for the VB states see **Figure S1**).[a]

Atom number				Torsion type	
#1	**#2**	**#3**	**#4**	**State 2**	**State 3**
14	13	17	18	1	1
14	13	17	19	1	0
15	13	17	18	1	1
15	13	17	19	1	0
16	13	17	18	1	1
16	13	17	19	1	0
17	13	14	19	0	1
15	13	14	19	0	1
16	13	14	19	0	1
2	4	5	8	14	14
2	4	5	8	15	15
2	4	5	8	16	16
2	4	5	8	17	17
2	4	5	8	18	18
4	5	8	9	24	24
4	5	8	9	25	25
4	5	8	9	26	26
4	5	8	9	27	27
4	5	8	9	28	28
5	8	9	12	1	1

[a] See **Figure S1** for the atom numbering.

Table S29. Torsion types used to describe the covalent bonds of the reacting part of the system, for GTP hydrolysis *via* a substrate-assisted mechanism, using the VB states described in **Figure S2**.[a]

Atom number				Torsion type	
#1	**#2**	**#3**	**#4**	**State 1**	**State 2**
10	9	12	13	1	0
11	9	12	13	1	0
8	9	12	13	2	0
8	9	12	13	3	0
8	9	12	13	4	0
8	9	12	13	5	0
8	9	12	13	6	0
9	12	13	14	7	0
9	12	13	14	8	0
9	12	13	15	7	0
9	12	13	15	8	0
9	12	13	16	7	0
9	12	13	16	8	0
14	13	17	18	0	1
14	13	17	19	0	1
15	13	17	18	0	1
15	13	17	19	0	1
16	13	17	18	0	1
16	13	17	19	0	1
2	4	5	8	9	14
2	4	5	8	10	15
2	4	5	8	11	16
2	4	5	8	12	17
2	4	5	8	13	18
4	5	8	9	19	24
4	5	8	9	20	25
4	5	8	9	21	26
4	5	8	9	22	27
4	5	8	9	23	28
5	8	9	12	2	0
5	8	9	12	3	0
5	8	9	12	4	0
5	8	9	12	5	0
5	8	9	12	6	1

[a] See **Figure S2** for the atom numbering.

S4. References

1. Duarte, F.; Åqvist, J.; Williams, N. H.; Kamerlin, S. C. L., Resolving Apparent Conflicts Between Theoretical and Experimental Models of Phosphate Monoester Hydrolysis. *J. Am. Chem. Soc.* **2014,** *137*, 1081-1093.

2. McGibbon, R. T.; Beauchamp, K. A.; Harrigan, M. P.; Klein, C.; Swails, J. M.; Hernández, C. X.; Schwantes, C. R.; Wang, L. P.; Lane, T. J.; Pande, V. J., MDTraj: A Modern Open Library for the Analysis of Molecular Dynamics Trajectories. *Biophys. J.* **2015,** *109*, 1528-1532.

3. Scheffzek, K.; Ahmadian, M. R.; Kabsch, W.; Wiesmuller, L.; Lautwein, A.; Schmitz, F.; Wittinghofer, A., The Ras-RasGAP Complex: Structural Basis for GTPase Activation and its Loss in Oncogenic Ras Mutants. *Science* **1997,** *277*, 333-338.

4. Voorhees, R. M.; Schmeing, T. M.; Kelley, A. C.; Ramakrishnan, V. T., The Mechanism for Activation of GTP Hydrolysis on the Ribosome. *Science* **2010,** *835-838*.

5. Scheidig, A. J.; Burmester, C.; Goody, R. S., The Pre-Hydrolysis State of p21Ras in Complex with GTP: New Insights into the Role of Water Molecules in the GTP Hydrolysis Reaction of Ras-like Proteins. *Structure* **1999,** *7*, 1311-1324.

6. Coleman, D. E.; Berghuis, A. M.; Lee, E.; Linder, M. E.; Gilman, A. G., Structures of Active Conformations of Gi Alpha 1 and the Mechanism of GTP Hydrolysis. *Science* **1994,** *265*, 1405-1412.

7. Müller, M. P.; Peters, H.; Blümer, J.; Blankenfeldt, W.; Goody, R. S.; Itzen, A., The Legionella Effector Protein DrrA AMPylates the Membrane Traffic Regulator Rab1b. *Science* **2010,** *329*, 946-949.

8. Gavriljuk, K.; Gazdag, E.-M.; Itzen, Y.; Kötting, C.; Goody, R. S.; Gerwert, K., Catalytic Mechanism of a Mammalian Rab*RabGAP Complex in Atomic Detail. *Proc. Natl. Acad. Sci. U. S. A.* **2012,** *109*, 21348-21353.

9. Krengel, U.; Schlichting, I.; Scherer, A.; Schumann, R.; Frech, M.; John, J.; Kabsch, W.; Pai, E. F.; Wittinghofer, A., Three-Dimensional Structures of H-ras p21 Mutants: Molecular Basis for their Inability to Function as Signal Switch Molecules. *Cell* **1990,** *62*, 539-548.

10. Schweins, T.; Geyer, M.; Scheffzek, K.; Warshel, A.; Robert, K.; Wittinghofer, A., Substrate-Assisted Catalysis as a Mechanism for GTP Hydrolysis of p21Ras and Other GTP-Binding Proteins. *Nat. Struct. Biol.* **1995,** *2*, 36-44.

11. Lan, K. L.; Zhong, H.; Nanamori, M.; Neubig, R. R., Rapid Kinetics of Regulator of G-protein Signaling (RGS)-Mediated $G_{\alpha i}$ and $G_{\alpha o}$ Deactivation. *J. Biol. Chem.* **2000,** *275*, 33497-33503.

12. Kötting, C.; Gerwert, K., Time-Resolved FTIR Studies Provide Activation Free Energy, Activation Enthalpy and Activation Entropy for GTPase Reactions. *Chem. Phys.* **2004,** *307*, 227-232.

13. Barrozo, A.; Blaha-Nelson, D.; Williams, N. H.; Kamerlin, S. C. L., The Effect of Magnesium Ions on Triphosphate Hydrolysis. *Pure Appl. Chem.* **2017,** *89*, 715-727.

14. Baxa, M. C.; Haddadian, E. J.; Jumper, J. M.; Freed, K. F.; Sosnick, T. R., Loss of Conformational Entropy in Protein Folding Calculated Using Realistic Ensembles and its Implications for NMR-Based Calculations. *Proc. Natl. Acad. Sci. U. S. A.* **2014,** *111*, 15396-15401.

15. Berman, H. M.; Westbrook, J.; Feng, Z.; Gilliland, G.; Bhat, T. N.; Weissig, H.; Shindyalov, I. N.; Bourne, P. E., The Protein Data Bank. *Nucleic Acids Res.* **2000,** *28*, 235-242.

16. Mann, D.; Teuber, C.; Tennigkeit, S. A.; Schröter, G.; Gerwert, K.; Kötting, C., Mechanism of the Intrinsic Arginine Finger in Heterotrimeric G Proteins. *Proc. Natl. Acad. Sci. U. S. A.* **2016,** *113*, E8041-E8050.